Measuring theoretical and actual observation influence in the Met Office UKV: application to Doppler radial winds

Geophysical Research Letters

RESEARCH LETTER
10.1029/2020GL091110

Key Points:
- The most impactful observations could be the most harmful if they are not assimilated correctly
- A simple method is developed to estimate simultaneously the influence of the observations and the optimality
- The metrics are illustrated on the Met Office's UKV assimilation of Doppler Radial Winds

Supporting Information:
- Supporting Information S1

Correspondence to:
A. M. Fowler,
a.m.fowler@reading.ac.uk

Citation:
Fowler, A. M., Simonin, D., & Waller, J. A. (2020). Measuring theoretical and actual observation influence in the MET Office UKV: Application to Doppler radial winds. *Geophysical Research Letters*, *47*, e2020GL091110. https://doi.org/10.1029/2020GL091110

Received 2 OCT 2020
Accepted 9 NOV 2020
Accepted article online 16 NOV 2020

Measuring Theoretical and Actual Observation Influence in the Met Office UKV: Application to Doppler Radial Winds

A. M. Fowler[1,2], **D. Simonin**[3], and **J. A. Waller**[3]

[1]Department of Meteorology, University of Reading, Reading, UK , [2]National Centre for Earth Observation, University of Reading, Reading, UK, [3]MetOffice@Reading, Reading, UK

Abstract In numerical weather prediction it is important to objectively measure the value of the observations assimilated. However, methods such as the forecast sensitivity to observation impact and observing system experiments are difficult to apply to convective scale data assimilation (DA) systems such as the Met Office's UK Variable-resolution model (UKV). We develop a new method to estimate the influence of the observations on the analysis, acknowledging that the influence depends not only on the uncertainty in the observations and prior, but how well these are prescribed in the assimilation. Monitoring both the actual and theoretical observation influence can flag observations that are being assimilated incorrectly and quantify the harm caused to the analysis. By applying these new estimates of the observation influence to the assimilation of Doppler Radial Winds in the UKV system, we demonstrate their ability, along with expert knowledge, to inform the optimization of both the observation network and DA system.

Plain Language Summary When forecasting the weather, it is essential to regularly combine (assimilate) numerical models of the atmosphere with observations to ensure that the forecasts stay in line with reality. At the Met Office ~45,000 observations coming from a myriad of instruments are used every hour to constrain high-resolution forecasts over the United Kingdom. Within this work we develop a new method to quantify how valuable different types of observations are for constraining the forecast along with a metric to assess if they are being assimilated correctly. It is demonstrated how the combination of these two metrics can be used to guide changes to the observing network and assimilation system.

1. Introduction

The Met Office's UK Variable-resolution model (UKV) system (Tang et al., 2013) aims to provide detailed short-range forecasts over the UK region. The interior resolution of the UKV is 1.5 km, permitting the UKV to explicitly model convection giving more realistic forecasts of rainfall. To keep the model in line with reality, ~45,000 observations are assimilated every hour using incremental 4DVar (Milan et al., 2019). Observation types include those that provide high-resolution information not needed in the global system, for example, radar-based precipitation rate analysis (Jones & Macpherson, 1997; Macpherson, 2001), Doppler radial wind data (Simonin et al., 2014), and screen-level temperature and humidity data from roadside sensors.

An objective measure of the value of the observations assimilated is essential to ensure that they are being utilized optimally. For example, such a measure can be used to guide changes to the observation network, flag issues with the data assimilation system and assess changes to the way observations are assimilated. Two methods typically used to monitor the impact of observations in the Met Office's global system are Observation System Experiments (OSEs, e.g., Hilton et al., 2009) and Forecast Sensitivity to Observation impact (FSOI, Lorenc & Marriott, 2014). Unfortunately, neither are particularly suited to convective-scale forecasting. For the OSE's this is due to the difficulty in the verification of forecast performance due to the small-scale variability of rainfall (Gilleland et al., 2009), as well as the usual problems with the expense of such an approach. For the FSOI the problems are twofold. The first is the nonlinearity of the model, meaning the adjoint at the necessary scales is only valid for too limited a time. Second, the analysis normally used for validation is not independent for a short-term forecast; this necessitates the use of a subset of observations to validate the forecast, skewing the impact of the observations measured to those used for validation

(Buttery & Macpherson, 2018). If an ensemble is available, then the problem of a lack of suitable adjoint can be addressed by the ensemble FSOI (EFSOI) proposed by Kalnay et al. (2012). This has been applied to the Deutscher Wetterdienst's (DWD) convective-scale limited area forecasting model COSMO (Consortium for Small-scale Modelling) in combination with the localized ensemble transform Kalman filter KENDA (Kilometre-scale Ensemble Data Assimilation) by Sommer and Weissmann (2016) and subsequently Necker et al. (2018), although the problem of needing to validate against observations remains.

Due to the difficulty in quantifying the observation impact on the forecast in the UKV and the lack of a suitable ensemble framework we instead propose to study the influence of the observations on the analysis, which in turn provides insight into the impact of the observations on the forecast. The influence that the observations have on the analysis depends primarily on the uncertainty of the observations and the prior; that is, accurate observations that provide information in regions of high prior uncertainty should have a greater influence than inaccurate observations. However, the influence of the observations will also depend on how well the data are assimilated, for example, the accuracy of the assumed error statistics and the consistency of the observation operator. Within this paper we propose a method to estimate the theoretical influence of the observations assuming that the system is optimal, in addition to the actual influence, which will be sensitive to the accuracy of these assumptions. Monitoring of both the theoretical and actual observation influence can be used to identify observations which are being assimilated suboptimally and allow for the harm caused to the analysis to be inferred.

2. Observation Influence Measured by $E[J_b(\mathbf{x}^a)]$

In variational data assimilation the analysis is computed as the maximum a posterior probability state assuming the prior (background), $\mathbf{x}^b \in \mathbb{R}^n$, and observations, $\mathbf{y} \in \mathbb{R}^p$, are randomly drawn from the following Gaussian distributions, respectively: $\mathbf{x}^b \sim N(\mathbf{x}^t, \mathbf{B})$ and $\mathbf{y} \sim N(h(\mathbf{x}^t), \mathbf{R})$. $\mathbf{x}^t$ is the truth in state space, $h : \mathbb{R}^n \to \mathbb{R}^p$ is the (possibly nonlinear) mapping from the state variables to the observed variables and $\mathbf{B}$ and $\mathbf{R}$ are the prior and observation error covariance matrices, respectively. The data assimilation problem can therefore be formulated as finding the minimum of the following cost function:

$$\begin{aligned} J(\mathbf{x}) &= -\text{constant} \times \ln\left(P(\mathbf{x}|\mathbf{y})\right) \\ &= (\mathbf{x}-\mathbf{x}^b)^T\mathbf{B}^{-1}(\mathbf{x}-\mathbf{x}^b) + (\mathbf{y}-h(\mathbf{x}))^T\mathbf{R}^{-1}(\mathbf{y}-h(\mathbf{x})) \\ &= J_b(\mathbf{x}) + J_o(\mathbf{x}). \end{aligned} \tag{1}$$

An analytical expression for the analysis that minimizes (1) can then be given by

$$\mathbf{x}^a = \mathbf{x}^b + \mathbf{K}\mathbf{d}_b^o, \tag{2}$$

where $\mathbf{d}_b^o = \mathbf{y} - h(\mathbf{x}^b)$ is referred to as the innovation and

$$\mathbf{K} = \mathbf{B}\mathbf{H}^T(\mathbf{H}\mathbf{B}\mathbf{H}^T + \mathbf{R})^{-1} \tag{3}$$

is the Kalman gain matrix, which governs how much weight should be given to the innovation when updating the prior (Kalnay, 2003). $\mathbf{H}$ is the Jacobian of the observation operator linearized about the best estimate of the state. When the observation operator is nonlinear, the analysis given in (2) can be found iteratively by relinearizing $\mathbf{H}$ about successive estimates of the state.

A measure of the observation influence, *OI*, can then be defined as $E[J_b(\mathbf{x}^a)]$,

$$OI = E[(\mathbf{x}^a-\mathbf{x}^b)^T\mathbf{B}^{-1}(\mathbf{x}^a-\mathbf{x}^b)]. \tag{4}$$

OI measures the expected influence of the observations in pulling the analysis, $\mathbf{x}^a$, away from the prior estimate of the state, $\mathbf{x}^b$.

In an optimal system (i.e., the statistics of the data uncertainty are correctly specified, and the observation operator is close to linear) the total degrees of freedom is given by $E[J(\mathbf{x}^a)] = p$ (the number of observations) (Bennett et al., 1993; Talagrand, 1999), and the *OI* is equivalent to the degrees of freedom for signal. In this case, *OI* is bounded by 0 and p, and $E[J_o(\mathbf{x}^a)] = p - E[J_b(\mathbf{x}^a)]$ (known as the degrees of freedom for noise). Therefore, *OI*/p tells you the percentage of information constraining each degree of freedom that is coming from the observations versus the background on average. In an optimal system, *OI* saturating as the number of observations is increased could be a useful indicator of the amount of redundancy in the observations; however, in a suboptimal system this may be a misleading interpretation.

2.1. Theoretical Observation Influence

An analytical value for OI can be derived if all assumptions made when assimilating the data are correct (Rodgers, 2000; Talagrand, 1999). This is evaluated in Appendix A to be

$$OI^{\mathrm{Th}} = \mathrm{trace}(\mathbf{HK}). \tag{5}$$

This has a lower bound of 0 (when the observations have had no influence on the analysis) and an upper bound of p (when the analysis perfectly fits the observations). Typically, we would wish to derive the contribution to the total observation influence by just a subset of observations. Following Chapnik et al. (2006), suppose $\boldsymbol{\Pi} \in \mathbb{R}^{\mathrm{p}_i \times \mathrm{p}}$ projects the full set of p observations onto just one observational type with p_i values. Then assuming the errors of the subset of observations are uncorrelated with the rest of the observations,

$$OI^{\mathrm{Th}}_{\Pi} = \mathrm{trace}(\boldsymbol{\Pi}\mathbf{HK}\boldsymbol{\Pi}^{\mathrm{T}}) \tag{6}$$

provides the contribution to the total observation influence from the subset of the observations given by $\boldsymbol{\Pi}\mathbf{y}$.

Directly computing OI^{Th} is challenging due to the need to compute the full $\mathbf{K}$ even when only interested in a subset of observations. The Degrees of Freedom for Signal as given by (5) and (6) has previously been estimated by the Lanczos conjugate gradient method at the ECMWF (Cardinali et al., 2004; Fisher, 2003) and by a randomization method at Meteo-France, whereby the trace of $\mathbf{HK}$ is evaluated with a large sample of perturbed analyses (Brousseau et al., 2014; Chapnik et al., 2006; Desroziers et al., 2009)).

2.2. Actual Observation Influence

In deriving the OI^{Th} it is assumed that the innovation covariance, $E[\mathbf{d}^{\mathrm{o}}_{\mathrm{b}}(\mathbf{d}^{\mathrm{o}}_{\mathrm{b}})^{\mathrm{T}}]$, is given by $\mathbf{D} = \mathbf{HBH}^{\mathrm{T}} + \mathbf{R}$. In practice it is not possible to specify $\mathbf{B}$ and $\mathbf{R}$ exactly at all times and locations, so each will often exhibit large misspecifications. Assuming $E[\mathbf{d}^{\mathrm{o}}_{\mathrm{b}}(\mathbf{d}^{\mathrm{o}}_{\mathrm{b}})^{\mathrm{T}}] = \mathbf{D}$ can also be a poor assumption when the data are non-Gaussian, have biases that have not been adequately corrected, or there are unaccounted for correlations between the observations and prior.

Let $\widetilde{\mathbf{D}}$ be the true covariances of the innovation such that $\widetilde{\mathbf{D}} = E[\mathbf{d}^{\mathrm{o}}_{\mathrm{b}}(\mathbf{d}^{\mathrm{o}}_{\mathrm{b}})^{\mathrm{T}}]$, then the actual observation influence is

$$OI^{\mathrm{Ac}} = \mathrm{trace}(\mathbf{HK}\widetilde{\mathbf{D}}\mathbf{D}^{-1}), \tag{7}$$

see Appendix A. The derivation of OI^{Ac} makes no assumption about the nature of the distribution of the innovations, allowing for both unaccounted for biases and non-Gaussianity. OI^{Ac} has a lower bound of 0 but unlike OI^{Th} it has no upper bound.

The contribution to the total actual observation influence from a subset of observations defined as $\boldsymbol{\Pi}\mathbf{y}$ is given by

$$OI^{\mathrm{Ac}}_{\Pi} = \mathrm{trace}(\boldsymbol{\Pi}\mathbf{HK}\widetilde{\mathbf{D}}\mathbf{D}^{-1}\boldsymbol{\Pi}^{\mathrm{T}}). \tag{8}$$

3. Caveats in Interpreting the Difference Between Actual and Theoretical Observation Influence

Comparing the actual and theoretical OI allows not only for the influence of the observations to be assessed but also if they are having the correct influence. This information can then be used to guide improvements to the DA system. However, there are some caveats that should be noted when interpreting the difference between actual and theoretical observation influence.

3.1. Interpreting the Source of the Discrepancy

If the actual and theoretical OI do not match, this implies that $\widetilde{\mathbf{D}} \neq \mathbf{D}$. The reasons for this could lie in the misspecification of either the background or observation error statistics making it difficult to interpret the source of the discrepancy. We illustrate this using a simple numerical experiment, similar to those described in Waller, et al. (2016) and Fowler et al. (2018), in which a circular domain is discretized into $n = 32$ grid points. The $p = 16$ (evenly distributed) observations are made directly of the state variables. The true statistics of the prior and observations are unbiased and Gaussian, consistent with the DA theory; however, in assimilating the data the covariances are not correctly specified. The true and assumed

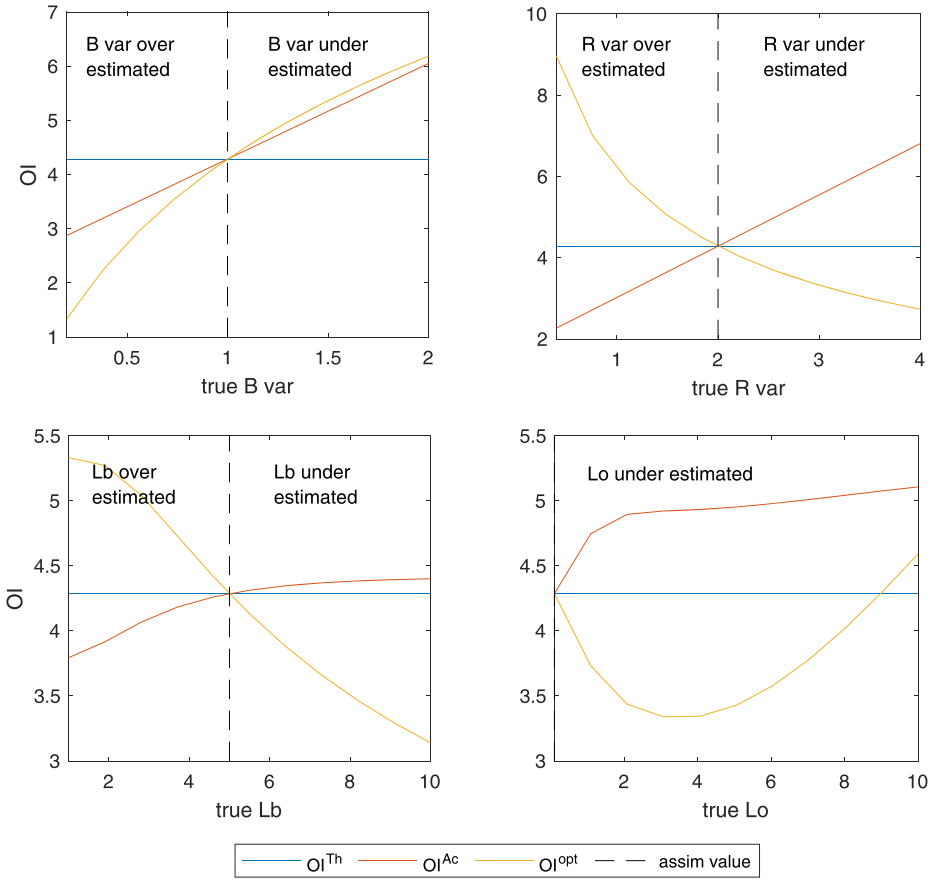

Figure 1. Theoretical *OI*, actual *OI*, and optimal *OI*, as a function of different parameters of the true error characteristics; background error variance (top left), observation error variance (top right), background correlation lengthscale (bottom left), observation error correlation lengthscale (bottom right). In each panel the vertical dashed line corresponds to the assumed value used in the assimilation. The true and assumed values only differ for the parameter being varied.

R and **B** are both generated using circulant matrices with second-order-autoregressive correlation functions, $c(k) = (1 + r_k/L)e^{-r_k/L}$, where L is the correlation lengthscale and r_k is the distance between two points. The assumed parameters for **R** and **B** are kept constant and given by 1 and 2 for the background and observation error variances, respectively, and 5 and 0.1 for the background and observation error correlation lengthscales (Lo and Lb), respectively.

In Figure 1 the theoretical, actual, and optimal (defined shortly) *OI* values are plotted as a function of the four true parameters. In each panel only one true parameter is varied with the others equal to the assumed values. Comparing (5) and (7) we see that the difference between OI^{Th} and OI^{Ac} depends upon $\widetilde{\mathbf{D}}\mathbf{D}^{-1}$, and hence makes no distinction between whether the misspecification is in **B** or **R**. We, therefore, see that the relationship between the theoretical and actual *OI* is similar in each of the following situations: if we underestimate (overestimate) the observation error variances, if we underestimate (overestimate) the background error variances or if we underestimate (overestimate) the correlation length-scales. That is, underestimating any of these parameters individually will result in the actual observation influence being greater than the theoretical value. Therefore, from the actual and theoretical observation influence alone it is impossible to say what the source of the discrepancy is. It is also therefore possible to make OI^{Ac} and OI^{Th} agree for the wrong reason as long as $\widetilde{\mathbf{D}} = \mathbf{D}$.

Despite this, attempts to use the discrepancy in the *OI* to objectively correct the error statistics used within the assimilation have been proposed with some success. Desroziers and Ivanov (2001), later modified by Chapnik et al. (2006), defined a scalar multiplication factor to tune the background error covariance matrix given by the ratio of the theoretical to actual $E[J_{\mathrm{b}}(\mathbf{x}^{\mathrm{a}})]$ for different subsets of the state variables.

The subsets were defined using the projection matrix $\mathbf{\Pi}^{\mathrm{b}}$ such that the theoretical $(E[J_{\mathrm{b}}(\mathbf{x}^{\mathrm{a}})])_{\mathbf{\Pi}^{\mathrm{b}}}$ becomes $Tr\left(\mathbf{\Pi}^{\mathrm{b}}\mathbf{KH}(\mathbf{\Pi}^{\mathrm{b}})^{\mathrm{T}}\right)$ using the permutation property of the trace of a product of matrices. $Tr\left(\mathbf{\Pi}^{\mathrm{b}}\mathbf{KH}(\mathbf{\Pi}^{\mathrm{b}})^{\mathrm{T}}\right)$ was evaluated using the randomization technique and the actual value of $E[J_{\mathrm{b}}(\mathbf{x}^{\mathrm{a}})]$ was evaluated using direct evaluation of $E[J_{\mathrm{b}}(\mathbf{x}^{\mathrm{a}})]$ for the same subsets of state variables over a representative sample. A similar multiplication for tuning $\mathbf{R}$ was also derived by the ratio of the actual to theoretical degrees of freedom for noise $E[J_{\mathrm{o}}(\mathbf{x}^{\mathrm{a}})]$ for different subsets of observations. Iterating these updates to $\mathbf{B}$ and $\mathbf{R}$ will help to align the theoretical and actual $E[J_{\mathrm{b}}(\mathbf{x}^{\mathrm{a}})]$ but will not guarantee an optimal Kalman gain matrix, $\mathbf{K}$, as seen in these simple experiments.

3.2. Inferring if Underfitting/Overfitting the Observations

Overfitting (underfitting) the observations can be defined as the optimal OI being less (more) than the actual OI, where the optimal OI is defined as

$$OI^{opt} = \mathrm{trace}(\mathbf{HK}^{opt}). \tag{9}$$

$\mathbf{K}^{opt}$ is the optimal Kalman gain matrix derived using the correct error covariance matrices. Equations 9 and 5 naturally have the same form, the difference being that $\mathbf{K}$ in (5) is derived from the covariances used within the assimilation. In practice OI^{opt} is never available and so we do not have the ability to directly compute if the observations are over or underfitted in this way. It would, therefore, be informative if the relationship between the theoretical and actual OI could be used to determine overfitting/underfitting to the observations. This would allow for the potential damage caused by not assimilating the observations correctly to be assessed; in that overfitting is potentially more damaging than underfitting. However, as well as not easily being able to use the discrepancy between OI^{Th} and OI^{Ac} to update the error covariance matrices, it is also difficult to use the discrepancy to make conclusions about whether you are overfitting or underfitting the observations. This is illustrated in Figure 1, where the optimal OI is given by the yellow lines. We see that the interpretation of the relationship between the theoretical and actual OI in terms of overfitting/underfitting depends on source of misspecification. For example, if it is just the background error variance that is misspecified then $OI^{\mathrm{Ac}} > OI^{\mathrm{Th}}$ implies that the observations are underfitted (although marginally in this example). However, if it is just the observation error variance that is misspecified, then $OI^{\mathrm{Ac}} > OI^{\mathrm{Th}}$ implies that the observations are overfitted.

Acknowledging these caveats, it is not recommended that the OI^{Th} and OI^{Ac} metrics are used to blindly make changes to the DA system. However, by providing valuable information about the quality/optimality of the DA system, they can be combined with expert knowledge of the instrument and assimilation system to guide changes.

4. Estimating Theoretical and Actual Observation Influence Using Observation-Model Misfits

Within this work we describe a new approach to estimate both the actual and theoretical observation influence using observation-model misfits. This approach has the benefit of being simpler to implement than previously proposed methods and not reliant on a particular architecture of the DA system. It also allows both the actual and theoretical observation influence to be partitioned into different subsets of observations and directly compared, which cannot be achieved when quantifying $E[J_{\mathrm{b}}(\mathbf{x}^{\mathrm{a}})]$ directly from the background part of the cost function in model space.

Let the analysis increments (in observation space) be defined as $\mathbf{d}^{\mathrm{a}}_{\mathrm{b}} = h(\mathbf{x}^{\mathrm{a}}) - h(\mathbf{x}^{\mathrm{b}})$. This can be written in terms of the innovation by approximating $h(\mathbf{x}^{\mathrm{a}}) - h(\mathbf{x}^{\mathrm{b}})$ as $\mathbf{H}|_{\mathbf{x}^{\mathrm{b}}}(\mathbf{x}^{\mathrm{a}} - \mathbf{x}^{\mathrm{b}})$, where $\mathbf{H}|_{\mathbf{x}^{\mathrm{b}}}$ is the nonlinear observation operator linearized about the background state. Substituting in the expression for the analysis (2) we find

$$\mathbf{d}^{\mathrm{a}}_{\mathrm{b}} = \mathbf{HK}\mathbf{d}^{\mathrm{o}}_{\mathrm{b}}. \tag{10}$$

Similarly, let the analysis residual be defined as $\mathbf{d}^{\mathrm{o}}_{\mathrm{a}} = \mathbf{y} - h(\mathbf{x}^{\mathrm{a}})$. This can be approximated as $\mathbf{d}^{\mathrm{o}}_{\mathrm{b}} - \mathbf{d}^{\mathrm{a}}_{\mathrm{b}}$, by replacing $h(\mathbf{x}^{\mathrm{a}})$ $(= h(\mathbf{x}^{\mathrm{b}} + \mathbf{K}\mathbf{d}^{\mathrm{o}}_{\mathrm{b}}))$ with $h(\mathbf{x}^{\mathrm{b}}) + \mathbf{H}|_{\mathbf{x}^{\mathrm{b}}}\mathbf{K}\mathbf{d}^{\mathrm{o}}_{\mathrm{b}}$. Therefore,

$$\mathbf{d}^{\mathrm{o}}_{\mathrm{a}} = (\mathbf{I}\text{-}\mathbf{HK})\mathbf{d}^{\mathrm{o}}_{\mathrm{b}}. \tag{11}$$

Note that $\mathbf{I\text{-}HK} = \mathbf{RD}^{-1}$ using (3).

The covariance of the analysis increment and residual can then be derived as

$$E[\mathbf{d}_b^a(\mathbf{d}_a^o)^T] = \mathbf{HK}\widetilde{\mathbf{D}}\mathbf{D}^{-1}\mathbf{R}. \tag{12}$$

In Desroziers et al. (2005) this is shown to provide an estimate of $\mathbf{HP}^a\mathbf{H}^T$, where $\mathbf{P}^a$ is the analysis error covariance matrix, when the assimilation system is optimal, that is, $\widetilde{\mathbf{D}} = \mathbf{D}$.

The covariance of the innovation and the analysis residual can similarly be derived as

$$E[\mathbf{d}_b^o(\mathbf{d}_a^o)^T] = \widetilde{\mathbf{D}}\mathbf{D}^{-1}\mathbf{R}. \tag{13}$$

In Desroziers et al. (2005) this is shown to provide an estimate of $\mathbf{R}$ when the assimilation system is optimal. Equation 13 has been used in many studies to infer the $\mathbf{R}$ matrix when the sources of uncertainty are multifarious (e.g., Stewart et al., 2013; Waller, Simonin, et al., 2016; Weston et al., 2014).

In the case when $\mathbf{R}$ contains off-diagonal elements or in the instance that $\mathbf{R}$ is parameterized differently from how we wish to stratify the influence metrics, it is beneficial to first normalize the residuals, innovations, and increments by $\mathbf{R}^{-1/2}$. For example, if the observation uncertainty is given as a function of the observed value, but we only wish to separate out the observation influence by position of the observation. Let $\hat{\mathbf{d}} = \mathbf{R}^{-1/2}\mathbf{d}$, then,

$$E\left[\hat{\mathbf{d}}_b^a(\hat{\mathbf{d}}_a^o)^T\right] = \mathbf{R}^{-1/2}\mathbf{HK}\widetilde{\mathbf{D}}\mathbf{D}^{-1}\mathbf{R}^{1/2}, \tag{14}$$

$$E\left[\hat{\mathbf{d}}_b^o(\hat{\mathbf{d}}_a^o)^T\right] = \mathbf{R}^{-1/2}\widetilde{\mathbf{D}}\mathbf{D}^{-1}\mathbf{R}^{1/2}. \tag{15}$$

Using (14) and (15) we can now derive estimates of the theoretical and actual observation influence:

$$OI^{Th} = \text{trace}\left(E\left[\hat{\mathbf{d}}_b^a(\hat{\mathbf{d}}_a^o)^T\right]\left(E\left[\hat{\mathbf{d}}_b^o(\hat{\mathbf{d}}_a^o)^T\right]\right)^{-1}\right) \tag{16}$$

$$OI^{Ac} = \text{trace}\left(E\left[\hat{\mathbf{d}}_b^a(\hat{\mathbf{d}}_a^o)^T\right]\right) \tag{17}$$

Note that the equalities in (16) and (17) only hold in the case of a linear observation operator. A discussion of highly nonlinear observation operators is given in the supporting information.

It is not necessary to remove biases from the vectors $\hat{\mathbf{d}}$ as we wish to include the effect of the unaccounted for biases in the true covariance of the innovations, $\widetilde{\mathbf{D}}$. This inconsistency with the assumptions made during the assimilation will therefore implicitly be present in the estimate of OI^{Ac} but is canceled out in the theoretical estimate when computed using (16).

Equations 16 and 17 can be derived from sample estimates of the covariances, assuming that the statistics do not vary over the sample.

$$OI^{Th} \approx \text{trace}\left(\sum_{i=1}^{N}\left(\hat{\mathbf{d}}_b^a\right)_i\left(\hat{\mathbf{d}}_a^o\right)_i^T\left(\sum_{i=1}^{N}\left(\hat{\mathbf{d}}_b^o\right)_i\left(\hat{\mathbf{d}}_a^o\right)_i^T\right)^{-1}\right) \tag{18}$$

$$OI^{Ac} \approx \text{trace}\left(\frac{1}{N-1}\sum_{i=1}^{N}\left(\hat{\mathbf{d}}_b^a\right)_i\left(\hat{\mathbf{d}}_a^o\right)_i^T\right) \tag{19}$$

where N is the sample size.

As the observation operator is linearized about the background, the Kalman gain matrix, in which the linearized observation operator appears, could potentially vary significantly over the sample. Therefore, selecting the sample and how to stratify the metrics needs careful consideration.

We see that normalizing the misfits by $\mathbf{R}^{-1/2}$ first acts to nondimensionalize the values. This has the benefit that, instead of dividing through by the sample estimate of $\widetilde{\mathbf{D}}\mathbf{D}^{-1}\mathbf{R}$ in (18), we divide through by the sample

estimate of $\mathbf{R}^{-1/2}\widetilde{\mathbf{D}}\mathbf{D}^{-1}\mathbf{R}^{1/2}$, which should be better conditioned (Tabeart et al., 2018). However, dividing through by the sample estimate of $\mathbf{R}^{-1/2}\widetilde{\mathbf{D}}\mathbf{D}^{-1}\mathbf{R}^{1/2}$ could still be problematic and make the estimate of the theoretical *OI* sensitive to the sample size and the assumptions made when constructing the off diagonal elements (e.g., ergodicity, isotropy, homogeneity). In addition to this we are only interested in a subset of the observations forcing us to assume $\mathbf{R}^{-1/2}\widetilde{\mathbf{D}}\mathbf{D}^{-1}\mathbf{R}^{1/2}$ is block diagonal so that

$$OI_{\boldsymbol{\Pi}}^{\mathrm{Th}} \approx \operatorname{trace}\left(E\left[\boldsymbol{\Pi}\hat{\mathbf{d}}_{\mathrm{b}}^{\mathrm{a}}(\boldsymbol{\Pi}\hat{\mathbf{d}}_{\mathrm{a}}^{\mathrm{o}})^{\mathrm{T}}\right]\left(E\left[\boldsymbol{\Pi}\hat{\mathbf{d}}_{\mathrm{b}}^{\mathrm{o}}(\boldsymbol{\Pi}\hat{\mathbf{d}}_{\mathrm{a}}^{\mathrm{o}})^{\mathrm{T}}\right]\right)^{-1}\right). \tag{20}$$

These concerns will be addressed in the next section in which the estimates of theoretical and actual *OI* are applied to the assimilation of Doppler radial winds.

To summarize, the proposed method provides a new way to measure the actual and theoretical influence of a subset of observations. Such metrics allow one to assess the validity of the assumptions made during the assimilation and to highlight observations that are potentially damaging to the analysis and hence the forecast. Computing these metrics from a sample of innovation and residual statistics means that they are easy to obtain for any DA system, as long as the observation operator is sufficiently linear. However, caution should be taken to ensure that the sample size is large enough to provide meaningful statistics with careful thought given to how the data are stratified.

5. Application to DRWs in the UKV

Doppler radial winds (DRWs) measured from weather radar provide high spatial and temporal estimates of wind in precipitating areas, making them vital for convective-scale forecasting (Simonin et al., 2014). The UK has a network of 18 C-Band weather radars each producing a plan position indicator (PPI) scan every 5 min at typically five different elevations, with a 1° by 600 m volume resolution. Two scanning strategies simultaneously produce rain fall and DRW estimates by mechanically moving the antenna to the desired elevations before each 360° scan. The five elevation angles have been chosen empirically to be 1°, 2°, 4°, 6°, and 9°. The mechanical nature of the scans means that the 5 min time constraint severely restricts the time available to perform any additional scans needed for quality control (e.g., a vertical dual polarization scan for reflectivity calibration or a linear depolarization ratio (LDR) scan used to detect the presence of the bright band). Application of the two *OI* metrics may provide a more objective argument to determine if these five elevation angles are all informative or if alternatively the number of elevations could be reduced, allowing for significantly more time for quality control with the associated benefits.

The data used for the following estimates of *OI* come from the test case used in Waller, Simonin, et al. (2016), in which the Desroziers et al. (2005) diagnostics, as in (13), were used to estimate correlated observation errors for the DRW. Archived observations, background, and resulting analysis data produced by the operational Met Office system are provided for June, July, and August 2013. At this time a 3DVar FGAT system with 3-hourly cycling was used to assimilate the data. Prior to assimilation, "superobservations" representing 3° × 3 km cells are calculated using the innovations following the method of Salonen et al. (2008). These are then further thinned to 6 km. The observation operator used to transform from the model variables to those observed interpolates the model horizontal and vertical wind components to the observation location. The horizontal wind is then projected in the direction of the radar beam and projected onto the slant of the radar beam. The observation operator therefore suffers from the following known inadequacies: (i) beam broadening and reflectivity weighting are unaccounted for, (ii) only the horizontal wind components are updated in the minimization, and (iii) no information about hydrometeor fall speed is available to the assimilation system. The observations are assumed to have uncorrelated errors with standard deviations given as a function of range only. These vary from 1.8 m s^{-1} close to the radar, and 2.8 m s^{-1} for observations farthest away from the radar. Further details of the operational assimilation of DRWs at this time at the Met Office can be found in Simonin et al. (2014).

Figures 2a and 2b show the sample size for each elevation, after quality control, during this 3 month period as a function of range and height, respectively. It can be seen that the majority of the data comes from the lower elevations due to these elevations producing more samples below the cloud top and hence in areas of precipitation. There is also a drop off in sample size at short range due to removal of ground clutter during quality control.

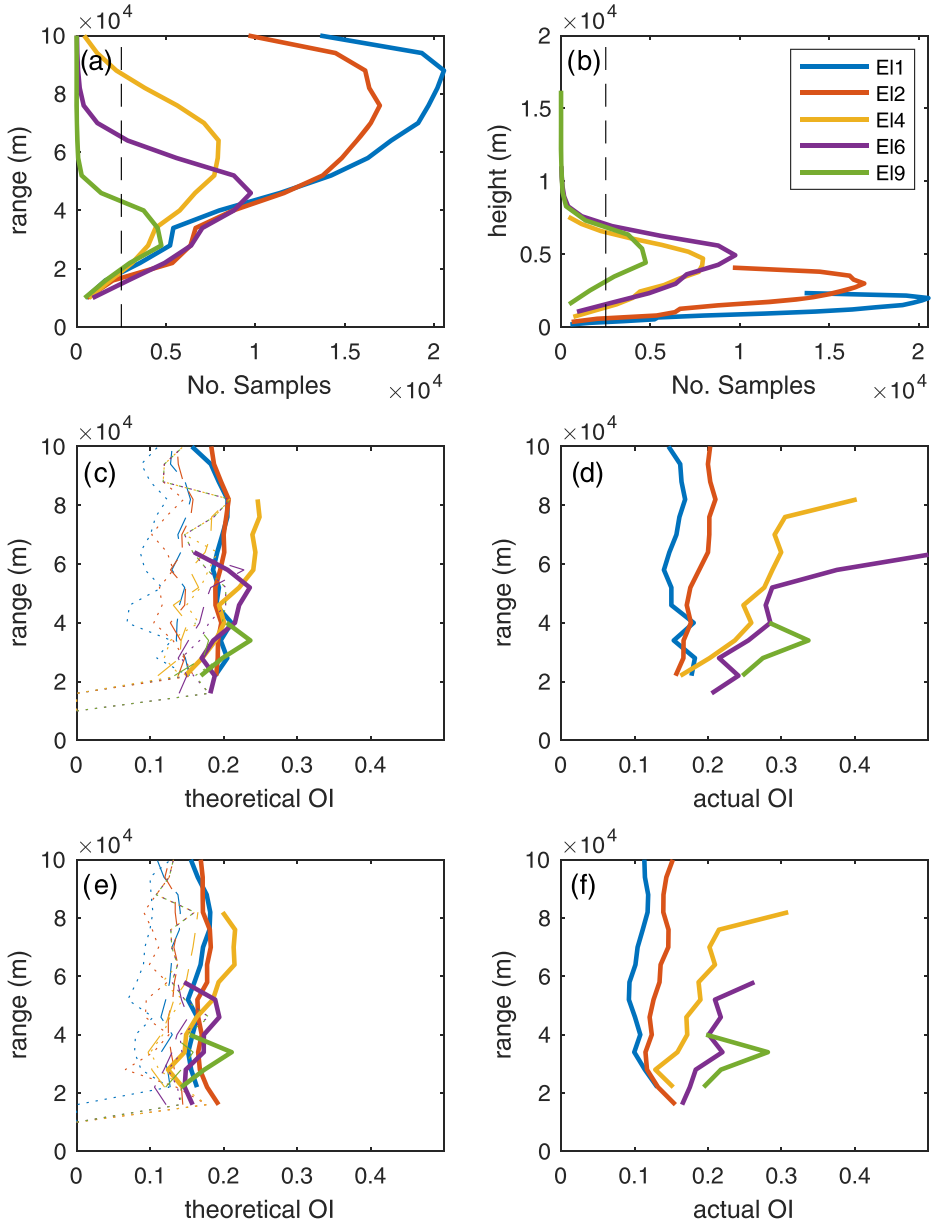

Figure 2. Number of samples for each elevation angle (see text; denoted El) as a function of (a) range and (b) height. The dashed line indicates the minimum sample size used to compute the sample estimates of *OI*. Sample estimates of (c, e) OI^{Th} and (d, f) OI^{Ac} are shown using (c, d) the old observation operator and (e, f) the new observation operator. Three different estimates of OI^{Th} are shown, see section 4, dotted lines: correlations in the data along the beam only are accounted for, dashed lines: correlations in the data on a horizontal plane only are accounted for, solid lines: no correlations in the data are accounted for.

Figures 2c and 2d show the sample estimates of the theoretical and actual *OI* for each elevation as a function of the range of the data. Values are only computed for sample sizes greater than 2,500.

For each elevation three estimates of OI^{Th} are provided depending on the assumptions made when reconstructing the sample estimate of $\mathbf{R}^{-1/2}\widetilde{\mathbf{D}}\mathbf{D}^{-1}\mathbf{R}^{1/2}$. Following Waller, Simonin, et al. (2016), the dotted lines are when it is assumed that the data are correlated along the beam only, the dashed line is when it is assumed that the data are correlated on a horizontal plane only, and the solid line is when it is assumed that the data are uncorrelated. Estimating the full $\mathbf{R}^{-1/2}\widetilde{\mathbf{D}}\mathbf{D}^{-1}\mathbf{R}^{1/2}$ (taking into account correlations across the full cone measured by the radar) is possible but would be very costly. Assuming $\mathbf{R}^{-1/2}\widetilde{\mathbf{D}}\mathbf{D}^{-1}\mathbf{R}^{1/2}$ is diagonal, although systematically overestimating OI^{Th} in this case, significantly reduces the computational cost of estimating

OI^{Th} and reduces the sensitivity of the estimate to the sampling noise. In general it is not clear if assuming $\mathbf{R}^{-1/2}\widetilde{\mathbf{D}}\mathbf{D}^{-1}\mathbf{R}^{1/2}$ is diagonal will underestimate or overestimate OI^{Th}, so a rough estimate of OI^{Th} attempting to include the covariances is useful for comparison.

From Figure 2c we can conclude that theoretically we would expect all elevations scanned to have proportionally similar influence on the analysis, which is reasonable given that similar assumptions are made when assimilating the data. Therefore, the total influence is proportional to the number of observations. If this were the only information available, then it may be concluded that the efficiency of the scanning strategy may be improved by only observing elevations 1° and 2°, as these have the most observations available (see Figures 2a and 2b) as well as perhaps elevation 6° to provide observations of wind higher in the atmosphere.

In contrast to Figure 2c, Figure 2d shows that the actual influence of the DRWs is greater for higher elevations and longer ranges. Based on OI^{Ac} only, it might instead be concluded that the efficiency of the scanning strategy may be improved by only observing elevations 4°, 6°, and 9° as elevations 1° and 2° have less weight per observation (or these lower elevations could be further thinned to reduce data redundancy at these levels). However, having both the estimates of OI^{Ac} and OI^{Th} allows for the conclusion that it is the observations that have the greatest actual influence (elevations 4° 6°, and 9°) that are assimilated using the poorest assumptions. Hence, these observations could be doing more harm than good. Based on both OI^{Ac} and OI^{Th}, a third conclusion might be that an improved analysis and forecast might be achieved if only elevations in which OI^{Ac} and OI^{Th} are aligned are assimilated, that is, elevations 1° and 2°.

This last hypothesis could be used to design data denial experiments; however, to some extent the difference between OI^{Ac} and OI^{Th} can be understood in terms of the validity of the observation operator and hence the validity of $\mathbf{R}$, which should account for uncertainty in the observation operator. The assumption that DRWs are a point estimate at the center of the beam becomes poorer as the range of the measurement is increased due to beam broadening. The linear interpolation from the model grid to the assumed point observation and the influence of vertical wind component also becomes worse as the elevation of the beam increases. We therefore have some confidence that the large difference in the actual and OI^{Th} is due to inadequacies in $\mathbf{R}$ rather than $\mathbf{B}$. From section 3.2 we can therefore speculate that when OI^{Ac} is greater than OI^{Th} the analysis is overfitting to the DRW observations.

An improved observation operator has been trialed, which accounts for some broadening of the beam (vertical only) as well as reflectivity weighting (Waller, Simonin, et al., 2016). Improving the observation operator has been shown to reduce the representation uncertainty (and error correlation), making the assumed observation error covariance matrix used within the assimilation more consistent with the data. This is seen by the improved agreement between OI^{Ac} and OI^{Th} plotted in Figures 2e and 2f) when recalculated using the new observation operator.

In initial trials, in which beam broadening was included within the observation operator, it has proven difficult to show significant benefit in the forecast verification. This could perhaps be expected due to the difficulty in obtaining validation statistics at the convective scales (Gilleland et al., 2009) and is why the use of objective consistency diagnostics such as the ones proposed here are so informative. However, the forecast trials did show some evidence of a degradation of the surface wind innovation when using the new observation operator, which may possibly be attributed to the length scales in the B matrix being too broad in the vertical and erroneously spreading the information in the DRWs to the surface. Hence, the new observation operator has not yet been implemented. The degradation of the surface winds could perhaps also have been monitored by applying the *OI* statistics to surface observations while making the changes to the way DRW observations are assimilated. It is therefore suggested that, when using these diagnostics to evaluate changes to the assimilation of one observation type, they are computed for a range of observations for which the background equivalent may also be affected, intentionally or not.

As noted previously, there is a trade-off here between having a large enough sample to minimize sampling noise and having a sample that satisfies the assumptions that the statistics are nonvariant over the time spanned by the sample. Experiments looking at the sensitivity to the sample selected have been performed. For example, the 3 month sample was separated out into different individual storms that passed over the UK. We found that although there are some differences between the different time periods, the overall conclusions hold; the actual OI is always greater than the theoretical OI and the agreement is improved when the new observation operator is used.

Figures 2e and 2f shows that there is naturally room for further improvements beyond the updated observation operator. These include accounting for correlations in **R**, which are thought to be significant even with 6 km thinning (Waller, Simonin, et al., 2016). Correlated errors for DRWs have now been implemented in the UKV for DRW (Simonin et al., 2019). As the new **R** has been derived from the Desroziers et al. (2005) consistency diagnostics, the OI^{Ac} and OI^{Th} should be more consistent by design. The comparison of OI^{Ac} and OI^{Th} could also be used to reevaluate the use of superobservations, and the use of flow-dependent errors for both **B** and **R**.

6. Summary and Conclusions

When designing an efficient and effective assimilation system it is desirable for each observations type, on average, to have a large impact on the analysis and forecast. However, a large impact is only beneficial if the observations are assimilated correctly. An estimate of both the actual and theoretical observation influence can help flag observations that are being assimilated incorrectly and quantify the harm caused to the analysis. The combination of these two metrics can allow for more informed decisions to be made regarding changes to the assimilation system.

We have demonstrated a simple method for estimating these two quantities from a sample of observations, background and analyses. The method is a natural by-product of the Desroziers et al. (2005) consistency diagnostics, which have been used extensively for estimating error covariance matrices for a variety of instruments. The method only relies on having a large enough sample of the inputs and outputs of the DA system and hence could be easily applied to any DA system based on Gaussian assumptions. The only constraint is that the mapping from the the model variables to those observed is near linear with respect to the magnitude of the analysis increments (see supporting information).

The *OI* metrics have been applied to the assimilation of DRWs using the Met Office's UKV system. It was shown that observations made at high elevations and long range have a much larger influence than they should theoretically have. This discrepancy could be explained in terms of the poor assumptions made by the observation operator and was confirmed by recomputing the diagnostics with an improved observation operator. This illustrated the potential of these metrics to be used to guide changes and improvements to a DA system cheaply.

The metric has also been applied to other observation types assimilated with the UKV, such as radiosonde measurements of temperature and humidity, atmospheric motion vectors derived from observations from the Spinning Enhanced Visible and Infrared Imager and radar reflectivities. Initial results show that these metrics provide useful information for these other observation types too, with the exception of the reflectivities where negative values were computed most likely due to the highly nonlinear observation operator.

Appendix A: Derivation of Theoretical and Actual Observation Influence

Substituting in the expression for the analysis (2) into (4), we can derive an analytical expression for *OI*. To simplify notation first let $\widetilde{\mathbf{D}} = E[\mathbf{d}_{\mathrm{b}}^{\mathrm{o}}(\mathbf{d}_{\mathrm{b}}^{\mathrm{o}})^{\mathrm{T}}]$ and $\mathbf{D} = \mathbf{H}\mathbf{B}\mathbf{H}^{\mathrm{T}} + \mathbf{R}$ (the assumed covariance of $\mathbf{d}_{\mathrm{b}}^{\mathrm{o}}$).

$$OI = E\left[(\mathbf{K}\mathbf{d}_{\mathrm{b}}^{\mathrm{o}})^{\mathrm{T}}\mathbf{B}^{-1}\mathbf{K}\mathbf{d}_{\mathrm{b}}^{\mathrm{o}}\right] \tag{A1}$$

$$= E\left[\mathrm{trace}\left((\mathbf{K}\mathbf{d}_{\mathrm{b}}^{\mathrm{o}})^{\mathrm{T}}\mathbf{B}^{-1}\mathbf{K}\mathbf{d}_{\mathrm{b}}^{\mathrm{o}}\right)\right] \tag{A2}$$

$$= E\left[\mathrm{trace}\left(\mathbf{d}_{\mathrm{b}}^{\mathrm{o}}(\mathbf{d}_{\mathrm{b}}^{\mathrm{o}})^{\mathrm{T}}\mathbf{K}^{\mathrm{T}}\mathbf{B}^{-1}\mathbf{K}\right)\right] \tag{A3}$$

$$= \mathrm{trace}\left(E\left[\mathbf{d}_{\mathrm{b}}^{\mathrm{o}}(\mathbf{d}_{\mathrm{b}}^{\mathrm{o}})^{\mathrm{T}}\right]\mathbf{K}^{\mathrm{T}}\mathbf{B}^{-1}\mathbf{K}\right) \tag{A4}$$

$$= \mathrm{trace}\left(\widetilde{\mathbf{D}}\mathbf{K}^{\mathrm{T}}\mathbf{B}^{-1}\mathbf{K}\right) \tag{A5}$$

Using the definition for $\mathbf{K}$, (3), this becomes

$$OI = \text{trace}\left(\widetilde{\mathbf{D}}\mathbf{D}^{-1}\mathbf{H}\mathbf{B}\mathbf{B}^{-1}\mathbf{K}\right) \tag{A6}$$

$$= \text{trace}\left(\widetilde{\mathbf{D}}\mathbf{D}^{-1}\mathbf{H}\mathbf{K}\right). \tag{A7}$$

Using the cyclic property of the trace of a product of matrices, OI can equivalently be written as

$$OI = \text{trace}\left(\mathbf{H}\mathbf{K}\widetilde{\mathbf{D}}\mathbf{D}^{-1}\right). \tag{A8}$$

No assumptions have been made here in terms of the nature of the statistics of $\mathbf{d}_b^o$. The innovations may be non-Gaussian, biased, and correlations may exist between the background and observations. Equation A8 therefore gives us an expression for the actual OI, which we refer to as OI^{Ac}.

The data assimilation theory, however, is based on the assumption that $\mathbf{D}$ and $\widetilde{\mathbf{D}}$ are equal, and the system is optimal. This allows us to derive an expression for the theoretical OI if all assumptions were correct

$$OI^{Th} = \text{trace}(\mathbf{H}\mathbf{K}). \tag{A9}$$

Data Availability Statement

The data sets for this research are available from the Centre for Environmental Data Analysis (Waller et al., 2020).

Acknowledgments
A. F. received funding for this work through the Natural Environment Research Council's national capability funding for NCEO, award NE/R016518/1.

References

Bennett, A., Leslie, L., Hagelberg, C., & Powers, P. (1993). Tropical cyclone prediction using a barotropic model initialized by a generalized inverse method. *Monthly Weather Review*, *121*, 1714–1729.

Brousseau, P., Desroziers, G., Bouttier, F., & Chapnik, B. (2014). A posteriori diagnostics of the impact of observations on the AROME-France convective-scale data assimilation system. *Quarterly Journal of the Royal Meteorological Society*, *140*(680), 982–994. https://doi.org/10.1002/qj.2179

Buttery, H., & Macpherson, B. (2018). FSOI using an Observation-Based Error Norm for the Met Office UKV model. In *6th International Symposium on Data Assimilation, 5–9 March 2018*, Munich, Germany.

Cardinali, C., Pezzulli, S., & Andersson, E. (2004). Influence-matrix diagnostics of a data assimilation system. *Quarterly Journal of the Royal Meteorological Society*, *130*, 2767–2786. https://doi.org/10.1256/qj.03.205

Chapnik, B., Desroziers, G., Rabier, F., & Talagrand, O. (2006). Diagnosis and tuning of observational error in a quasi-operational data assimilation setting. *Quarterly Journal of the Royal Meteorological Society*, *132*(615), 543–565. https://doi.org/10.1256/qj.04.102

Desroziers, G., Berre, L., Chabot, V., & Chapnik, B. (2009). A Posteriori Diagnostics in an Ensemble of Perturbed Analyses. *Monthly Weather Review*, *137*(10), 3420–3436. https://doi.org/10.1175/2009MWR2778.1

Desroziers, G., Berre, L., Chapnik, B., & Poli, P. (2005). Diagnosis of observation, background and analysis-error statistics in observation space. *Quarterly Journal of the Royal Meteorological Society*, *131*(613), 3385–3396.

Desroziers, G., & Ivanov, S. (2001). Diagnosis and adaptive tuning of information error parameters in variational assimilation. *Quarterly Journal of the Royal Meteorological Society*, *127*, 1433–1452.

Fisher, M. (2003). Estimation of Entropy Reduction and Degrees of Freedom for Signal for Large Variational Analysis Systems. ECMWF.

Fowler, A., Dance, S., & Waller, J. (2018). On the interaction of observation and a-priori error correlations. *Quarterly Journal of the Royal Meteorological Society*, *144*, 48–62. https://doi.org/10.1002/qj.3183

Gilleland, E., Ahijevych, D., Brown, B. G., Casati, B., & Ebert, E. E. (2009). Intercomparison of Spatial Forecast Verification Methods. *Weather and Forecasting*, *24*(5), 1416–1430. https://doi.org/10.1175/2009WAF2222269.1

Hilton, F., Atkinson, N. C., English, S. J., & Eyre, J. R. (2009). Assimilation of IASI at the Met Office and assessment of its impact through observing system experiments. *Quarterly Journal of the Royal Meteorological Society*, *135*(639), 495–505. https://doi.org/10.1002/qj.379

Jones, C., & Macpherson, B. (1997). A latent heat nudging scheme for the assimilation of precipitation data into an operational mesoscale model. *Meteorological Applications*, *4*, 269–277.

Kalnay, E. (2003). *Atmospheric modeling, data assimilation and predictability*. New York: Cambridge University Press.

Kalnay, E., Ota, Y., Miyoshi, T., & Liu, J. (2012). A simpler formulation of forecast sensitivity to observations: application to ensemble Kalman filters. *Tellus A: Dynamic Meteorology and Oceanography*, *64*(1), 18462. https://doi.org/10.3402/tellusa.v64i0.18462

Lorenc, A. C., & Marriott, R. T. (2014). Forecast sensitivity to observations in the Met Office Global numerical weather prediction system. *Quarterly Journal of the Royal Meteorological Society*, *140*(678), 209–224. https://doi.org/10.1002/qj.2122

Macpherson, B. (2001). Operational experience with assimilation of rainfall data in the Met Office Mesoscale model. *Meteorology and Atmospheric Physics*, *76*, 3–8. https://doi.org/10.1007/s007030170035

Milan, M., Macpherson, B., Tubbs, R., Dow, G., Inverarity, G., Mittermaier, M., & Wlasak, M. (2019). Hourly 4D-Var in the Met Office UKV operational forecast model. *Quarterly Journal of the Royal Meteorological Society*, *146*, 1281–1301. https://doi.org/10.1002/qj.3737

Necker, T., Weissmann, M., & Sommer, M. (2018). The importance of appropriate verification metrics for the assessment of observation impact in a convection-permitting modelling system. *Quarterly Journal of the Royal Meteorological Society*, *144*, 1667–1680. https://doi.org/10.1002/qj.3390

Rodgers, C. D. (2000). *Inverse methods for atmospheric sounding*. Singapore: World Scientific Publishing.

Salonen, K., Jarvinen, H., Jarvenoja, S., Niemela, S., & Eresmaa, R. (2008). Doppler radar radial wind data in NWP model validation. *Meteorological Applications*, *15*(1), 97–102. https://doi.org/10.1002/met.47

Simonin, D., Ballard, S. P., & Li, Z. (2014). Doppler radar radial wind assimilation using an hourly cycling 3D-Var with a 1.5 km resolution version of the Met Office Unified Model for nowcastings. *Quarterly Journal of the Royal Meteorological Society*, *140*, 2298–2314. https://doi.org/10.1002/qj.2298

Simonin, D., Waller, J. A., Ballard, S. P., Dance, S. L., & Nichols, N. K. (2019). A pragmatic strategy for implementing spatially correlated observation errors in an operational system: An application to Doppler radial winds. *Quarterly Journal of the Royal Meteorological Society*, *145*(723), 2772–2790. https://doi.org/10.1002/qj.3592

Sommer, M., & Weissmann, M. (2016). Ensemble-based approximation of observation impact using an observation-based verification metric. *Tellus A: Dynamic Meteorology and Oceanography*, *68*(1), 27885. https://doi.org/10.3402/tellusa.v68.27885

Stewart, L. M., Dance, S. L., & Nichols, N. K. (2013). Data assimilation with correlated observation errors: experiments with a 1-D shallow water model. *Tellus A*, *65*, 19,546.

Tabeart, J. M., Dance, S. L., Haben, S. A., Lawless, A. S., Nichols, N. K., & Waller, J. A. (2018). The conditioning of least-squares problems in variational data assimilation. *Numerical Linear Algebra with Applications*, *25*, e2165. https://doi.org/10.1002/nla.2165

Talagrand, O. (1999). A posteriori verification of analysis and assimilation algorithms. In *Proc. ECMWF Workshop on Diagnosis of Data Assimilation Systems* (pp. 17–28). Reading, United Kingdom: ECMWF.

Tang, Y., Lean, H. W., & Bornemann, J. (2013). The benefits of the Met Office variable resolution NWP model for forecasting convection. *Meteorological Applications*, *20*(4), 417–426. https://doi.org/10.1002/met.1300

Waller, J. A., Dance, S. L., & Nichols, N. K. (2016). Theoretical insight into diagnosing observation error correlations using observation-minus-background and observation-minus-analysis statistics. *Quarterly Journal of the Royal Meteorological Society*, *142*, 418–431.

Waller, J. A., Simonin, D., Dance, S. L., Nichols, N. K., & Ballard, S. P. (2016). Diagnosing observation error correlations for Doppler radar radial winds in the Met Office UKV model using observation-minus-background and observation-minus-analysis statistics. *Monthly Weather Review*, *144*, 3533–3551. https://doi.org/10.1175/MWR-D-15-0340.1

Waller, J., Simonin, D., Dance, S., Nichols, N., & Ballard, S. (2020). FRANC: Doppler radar radial wind observations and associated observation-minus-model residuals from the Met Office UKV 3D Var assimilation scheme. Centre for Environmental Data Analysis, https://doi.org/10.5285/5d8221e070e64823891bed7a87840447

Weston, P. P., Bell, W., & Eyre, J. R. (2014). Accounting for correlated error in the assimilation of high-resolution sounder data. *Quarterly Journal of the Royal Meteorological Society*, *140*, 2420–2429.